Supplementary Materials and Methods

***Reagents*.** GW3965 and other nuclear receptor ligands were provided by T. Willson (GlaxoSmithKline). HSC-T6 and LX-2 cell lines were kindly provided by Scott Friedman. Purified LPS came from Alexis Biochemicals, Pronase from Roche, OptiPrep density gradient from Axis-Shield, and BODIPY from Invitrogen. All other enzymes, antibodies, and chemicals were from Sigma-Aldrich.

Primary stellate cell isolation protocol. Briefly, the liver is flushed *in situ* with a chelating solution of EMEM + 1% EGTA for 5 minutes, followed by perfusion with 0.5 - 0.7% Pronase for 16-20 minutes, followed by 0.4% collagenase for 5-8 minutes. The digested liver is then further incubated with an DNAse (10 μg/mL) for 10 min at 37°C. After removal of debris and hepatocytes by low speed centrifugation (600g x 1 minute), the nonparenchymal fraction is pelleted (2300g x 7 minutes). Cells are resuspended and purified by ultracentrifugation over a discontinuous density gradient (OptiPrep) at 12,000g x 15 minutes. Stellate cells are collected from the lightest density layers (1.034 - 1.043 g/cm^3), washed, and seeded onto culture dishes in low glucose DMEM with 10% FBS and antibiotics. Purity of stellate cells was determined to be 97+% pure at the time of isolation. Confirmation of retinoid content is observed by rapidly fading autofluorescence upon excitation by UV light.

Tissue, serum, and histologic analysis. Animals were fasted for 6 hours before sacrifice and blood collected by cardiac puncture with serum separated by centrifugation at 8000 rpm for 5 minutes, 4°C. Alanine aminotransferase was determined by standard colorimetric analysis. The largest lobe of the liver was preserved for 24-48 hours in 10% w/v formalin and then transferred to 50% ethanol and kept at 4°C until sectioned. Masson's trichrome staining and unstained slides were prepared by our core facilities (UCLA Translational Pathology Core Laboratory).

Immunohistochemical staining was performed on paraffin embedded sections cut 4 microns thick. Slides were pressure cooked for antigen retrieval and then labeled with a primary monoclonal antibody to α-smooth muscle actin (A5228, lot 087K4775, Sigma). Secondary antibodies were anti-mouse horseradish peroxidase.

Digital quantification of fibrosis. Photomicrographs of sections were obtained using a ScanScope XT System (Aperio Technologies, Inc., Vista, CA) at a magnification of 200X. Sections were then scanned and analyzed using the Ariol SL-50 automated slide scanner (Applied Imaging, San Jose) to quantitate the amount of fibrotic material for each tissue slice. Thresholds for each image were applied using the Ariol analytical software based on multiple parameters: RGB algorithm, shape and size. All analyses were performed with the MultiStain script. For assessing staining, the area of positive stain was calculated by applying color thresholds to detect positive blue pixels. Percent of positivity was determined by dividing the total positive stain area (μm^2) by the total tissue area analyzed (μm^2). Scanning and analyses were performed through the UCLA Translational Pathology Core Laboratory.

FACS Phenotyping and Cell Proliferation Assay*.* Non-parenchymal cells from up to four mice were isolated by *in situ* Pronase / collagenase digestion and pooled for extensive characterization by FACS phenotyping. Initially, we gated the FACS analysis to exclude small particles (debris and apoptotic bodies) and large clumps (hepatocytes and non-digested material). In the remaining population we identified significant populations of B, T, NKT, macrophages (both inactive and activated), and endothelial cells, as well as cells that showed evidence of autofluorescence upon DAPI excitation. We then employed a negative depletion strategy by using specific antibodies directed at CD3 (T cell), CD19 & B220 (B cell), CD31 (endothelial) MHC II (immune and macrophage), and DX-5 (NKT) epitopes to deplete those cell populations over magnetic bead columns (MACS Bead System, Miltenyi). The resulting

population of non-parenchymal cells displayed evidence of autofluorescence in FACS analysis and appeared to be morphologically similar to hepatic stellate cells, including the presence of lipid droplets with autofluorescence. These cells were plated on plastic and proliferated over several days of culture activation with the absence of B, T, macrophage, and endothelial markers by qPCR. They also showed marked upregulation of expected stellate cell markers, including fibrotic genes, inflammatory cytokines, and the transcription factor KLF6, known to regulate stellate cell activation. After phenotyping, we conducted separate experiments in which we treated this cell population with LXR ligands for seven days before trypsinizing and comparing the number of live cells in flow cytometry as a measure of cellular proliferation.

Supplementary Figure Legends

Supplementary Figure 1. LXRs, unlike PPARγ and FXR, are functionally expressed in immortalized stellate cells. (A) Human LX-2 cells were treated with specific nuclear receptor agonists for RXR, RARα, PPARγ, and FXR (100-500 nM). 12-16 hours later, cells were harvested and analyzed by qPCR for gene expression of AP2 (PPARγ target) or SHP (FXR target). These target genes were only detected at extremely high Ct values, with significant variation in expression levels. **(B)** Gene expression by qPCR of LXRα and LXRβ during culture activation of primary stellate cells from WT mice.

Supplementary Figure 2. LXR agonists are anti-proliferative on the non-parenchymal hepatic fraction. Non-parenchymal fractions were isolated as described (cf. Supplementary Methods) from pairs of WT and *Lxr*αβ-/- mice and depleted of B cells, T cells, macrophages, endothelial cells, and NKT cells using the MACS bead system. Resulting populations were plated directly on plastic and treated with 1 μM GW3965 for seven days. Significant cell toxicity was not observed. On the seventh day, cells were trypsinized and analyzed by flow cytometry to identify live cells (100,000 events counted).

Supplementary Figure 3. Synthetic LXR ligands have reciprocal anti-inflammatory and lipogenic effects in primary WT stellate cells. Additional gene expression by qPCR and time points to Figure 3C are shown for WT primary stellate cells treated continuously with either 1 μM T0901317 (abbreviated T1317) or vehicle (DMSO) throughout culture activation.

Supplementary Figure 4. Oxysterols regulate inflammatory and lipogenic gene expression in primary WT stellate cells. Stellate cells were purified from WT mice (cf

Methods) and plated on plastic for a culture activation model. On day 2 after isolation, media was replaced with DMEM containing 1% FBS, pen/strep/ampho supplemented with 5 μM simvastatin and 100 μM mevalonic acid to quench endogenous sterol and oxysterol production. Eight hours later cells were incubated with vehicle (EtOH), 1 μM 22(R)-hydroxycholesterol, or its inactive enantiomer, 22(S)-hydroxycholesterol, for another 16 to 64 h. Gene expression by qPCR for canonical LXR targets (*Abca1*, *Srebp-1c*) and stellate cell inflammatory (*Mcp1 and Il-6*) and activation related genes (*Tgfβ1*, *Klf6*) is shown. N.B. The loss of effect on *Srebp-1c* at day 5 is not unexpected, since *Srebp-1c* expression is auto-regulated and oxysterols block the cleavage of Srebp-1c into its active form.

Supplementary Figure 5. LXR null mice have a subtle increase in basal levels of fibrosis. WT and *Lxrαβ*-/- livers, N = 11 per genotype, were harvested at 16 weeks of age and sections prepared for Masson's trichrome staining without any injury stimulus beforehand. Quantified hepatic fibrosis by digital scanning is shown. Statistical analysis by Student's *t* test: ***, $P < .001$.

Supplementary Figure 6. Markers of hepatocellular injury and CCl_4 biotransformation during chronic injury. (A) qPCR gene expression of *Cyp2e1*, the enzyme which metabolizes CCl_4 into its hepatoxic form, in WT and *Lxrαβ*-/- animals chronically treated with CCl_4 (N=10 per group). **(B)** Alanine aminotransferase (ALT) levels after chronic CCl_4 treatment in the reciprocal bone marrow transplants. **(C)** qPCR gene expression of *Cyp2e1* in wild-type recipient chimeras after chronic CCl_4 or vehicle, (N=8-10 per group).

Nuclear Receptor	Relative Abundance in LX2 Cells by qPCR
LXRα	+
LXRβ	+++
PPARα	++
PPARγ	-
PPARδ	++
FXR	-
PXR	-
CAR	-
Vitamin D Receptor	+++
Thyroid (TRα, TRβ) Receptors	+++
RARα	++
RARβ	-
RARγ	-
RXRα	++
RXRβ	-

Supplemental Table 1. Relative abundance of RXR heterodimers in human LX-2 stellate cells. As measured by quantitative real-time PCR, '+++' indicates Ct values < 25, '++' Ct = 25-30, and '+' Ct = 30-35. A '–' indicates no significant expression by qPCR (Ct > 35).

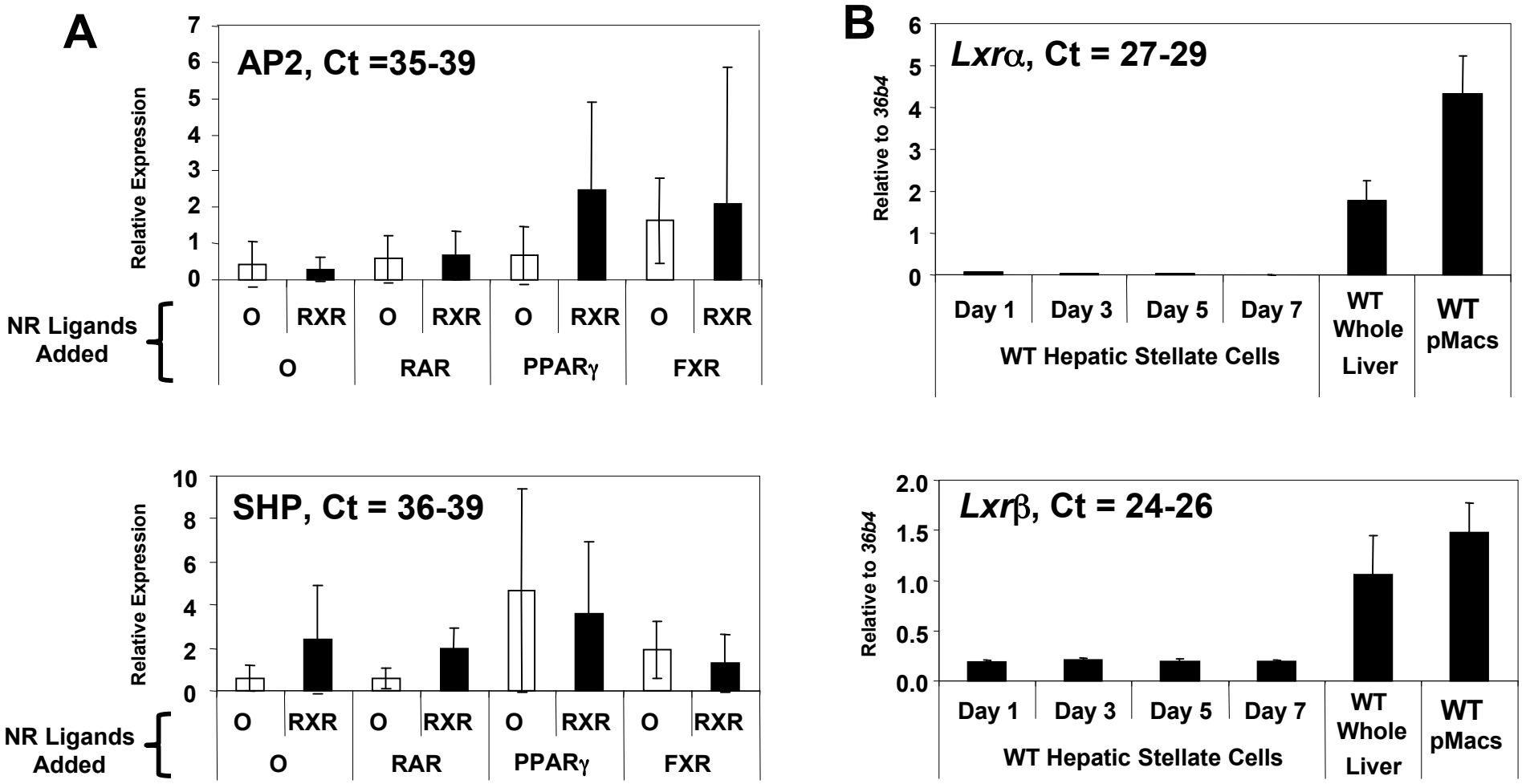

Beaven Suppl Figure 1

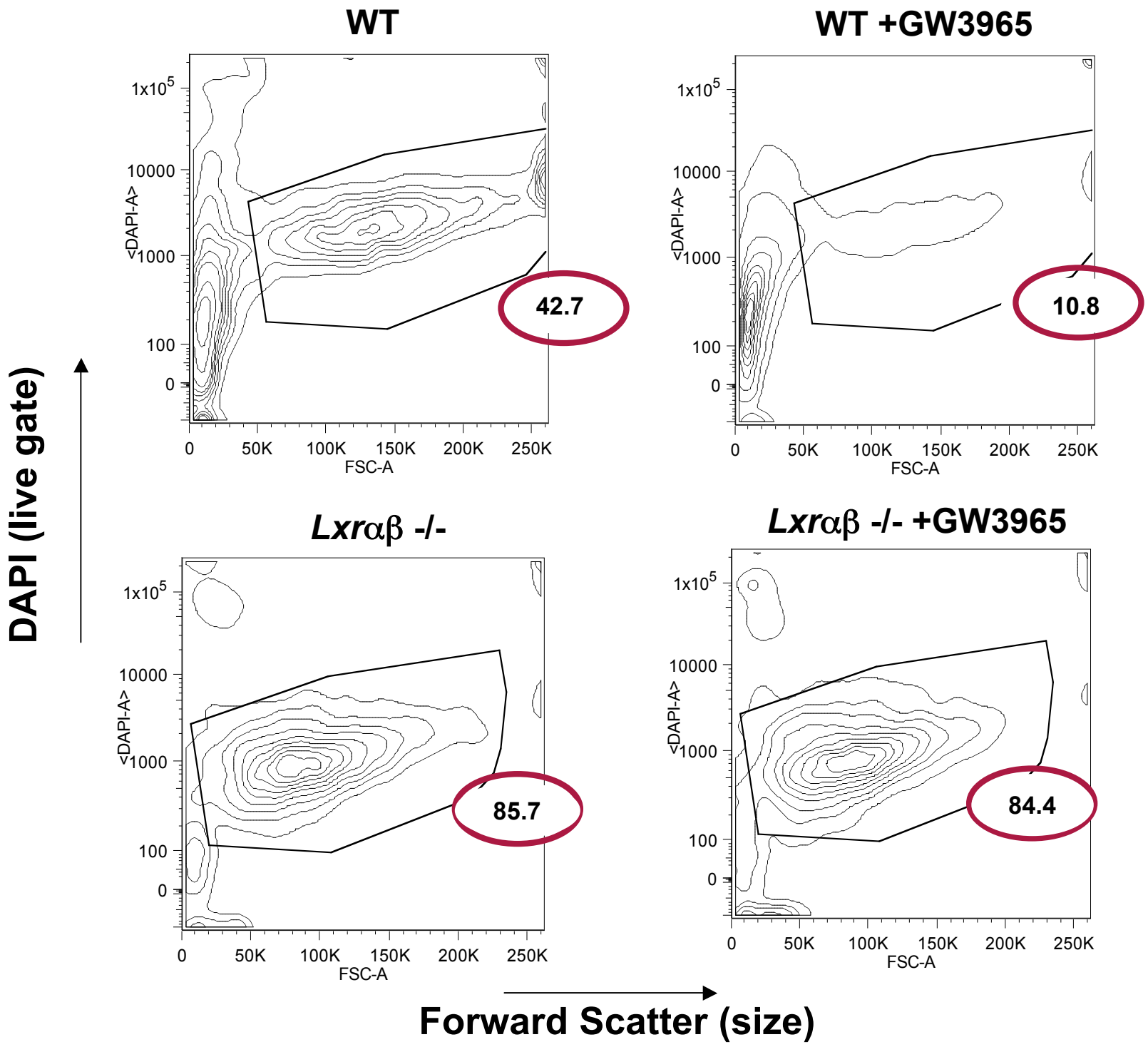

Beaven Suppl Figure 2

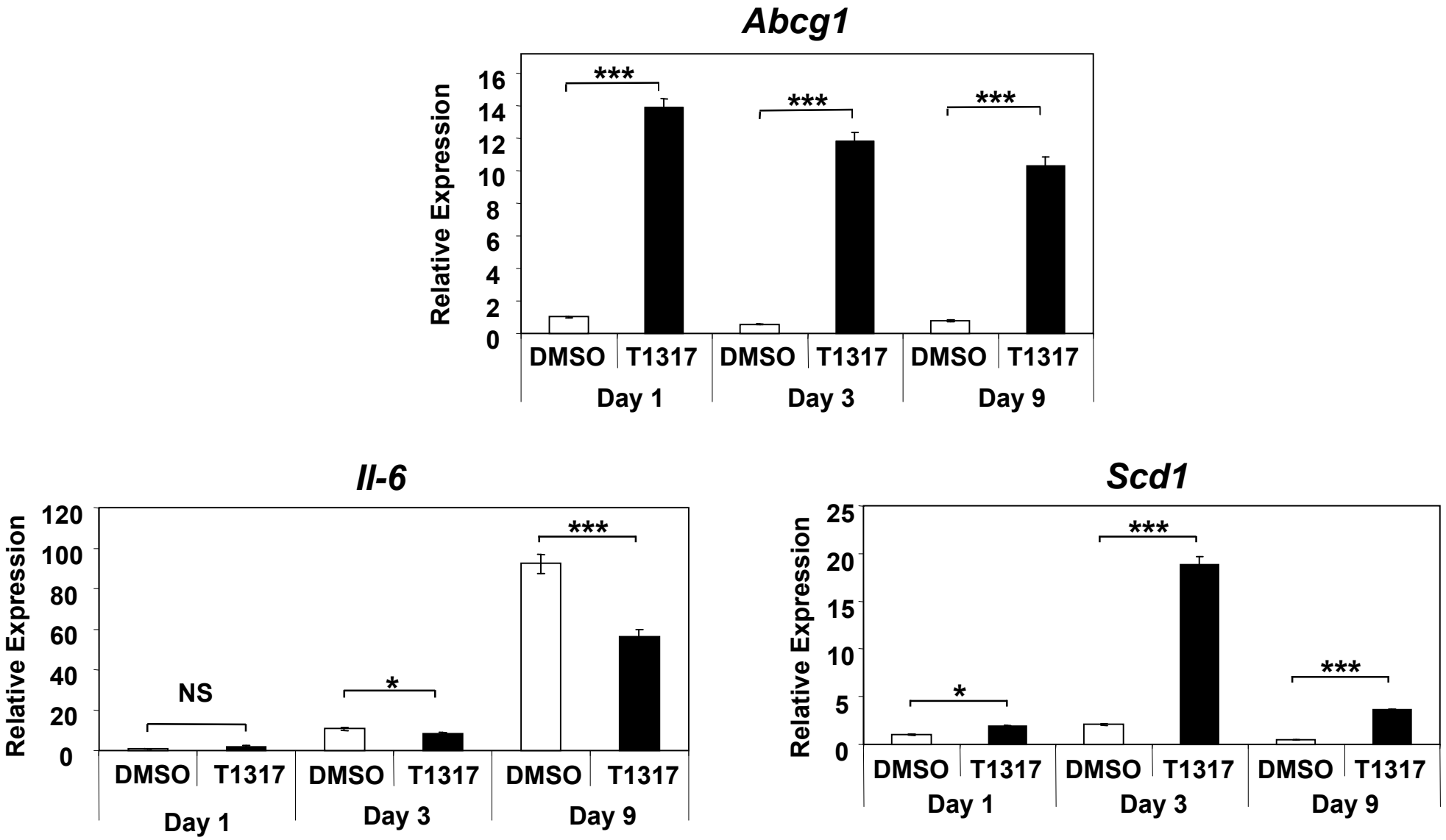

Beaven Suppl Figure 3

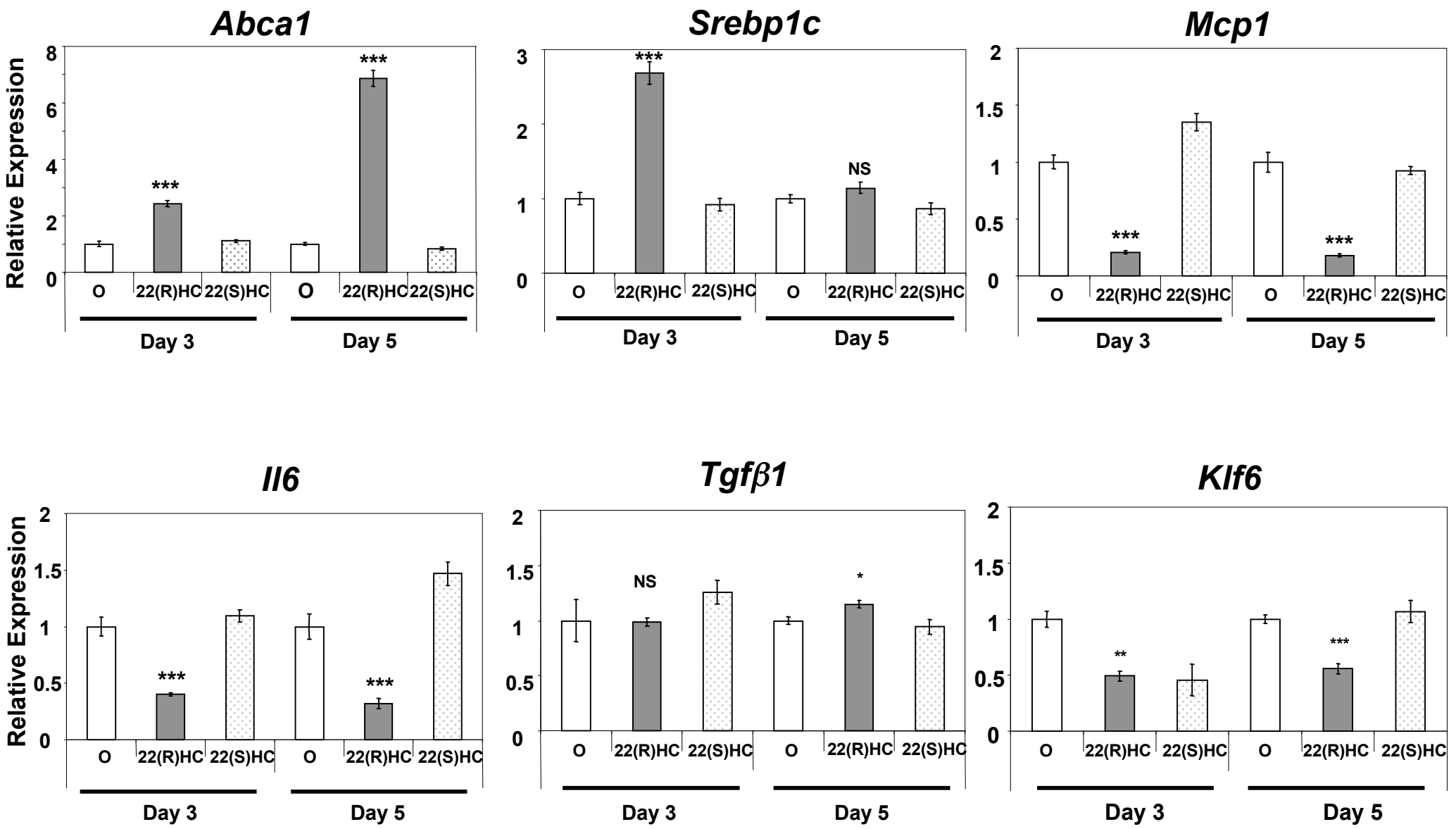

Beaven Suppl Figure 4

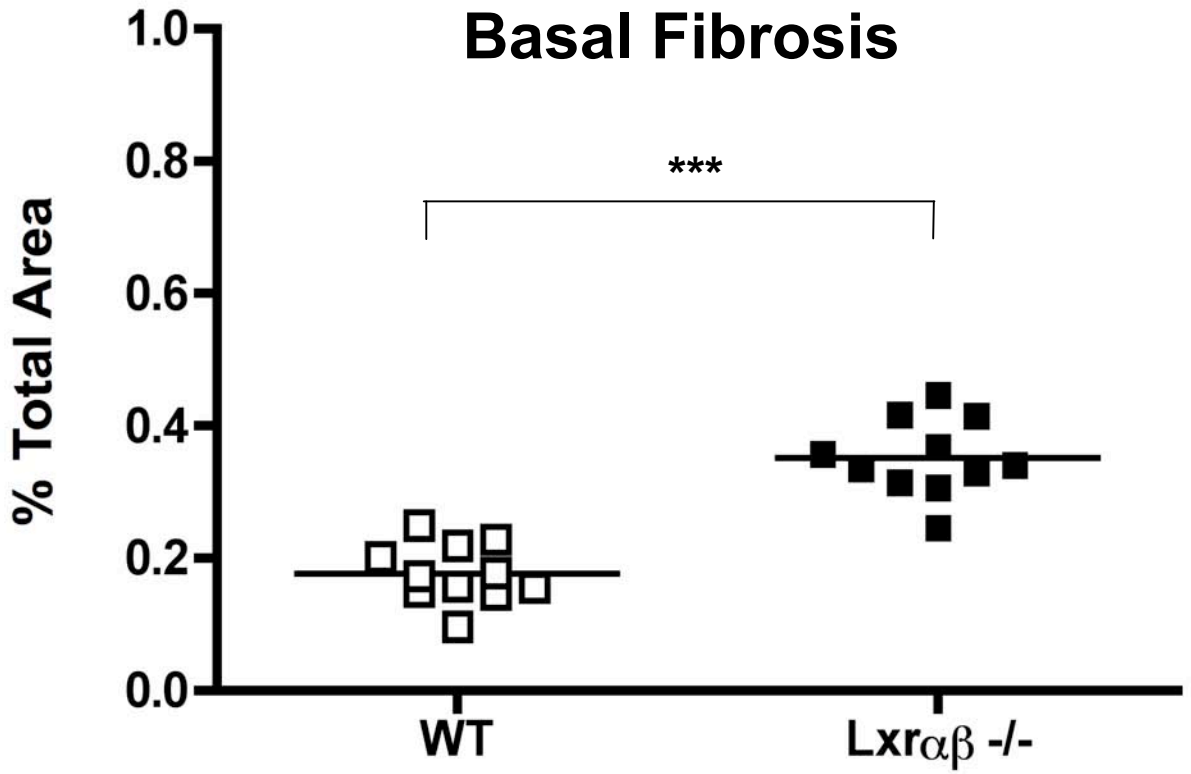

Beaven Suppl Figure 5

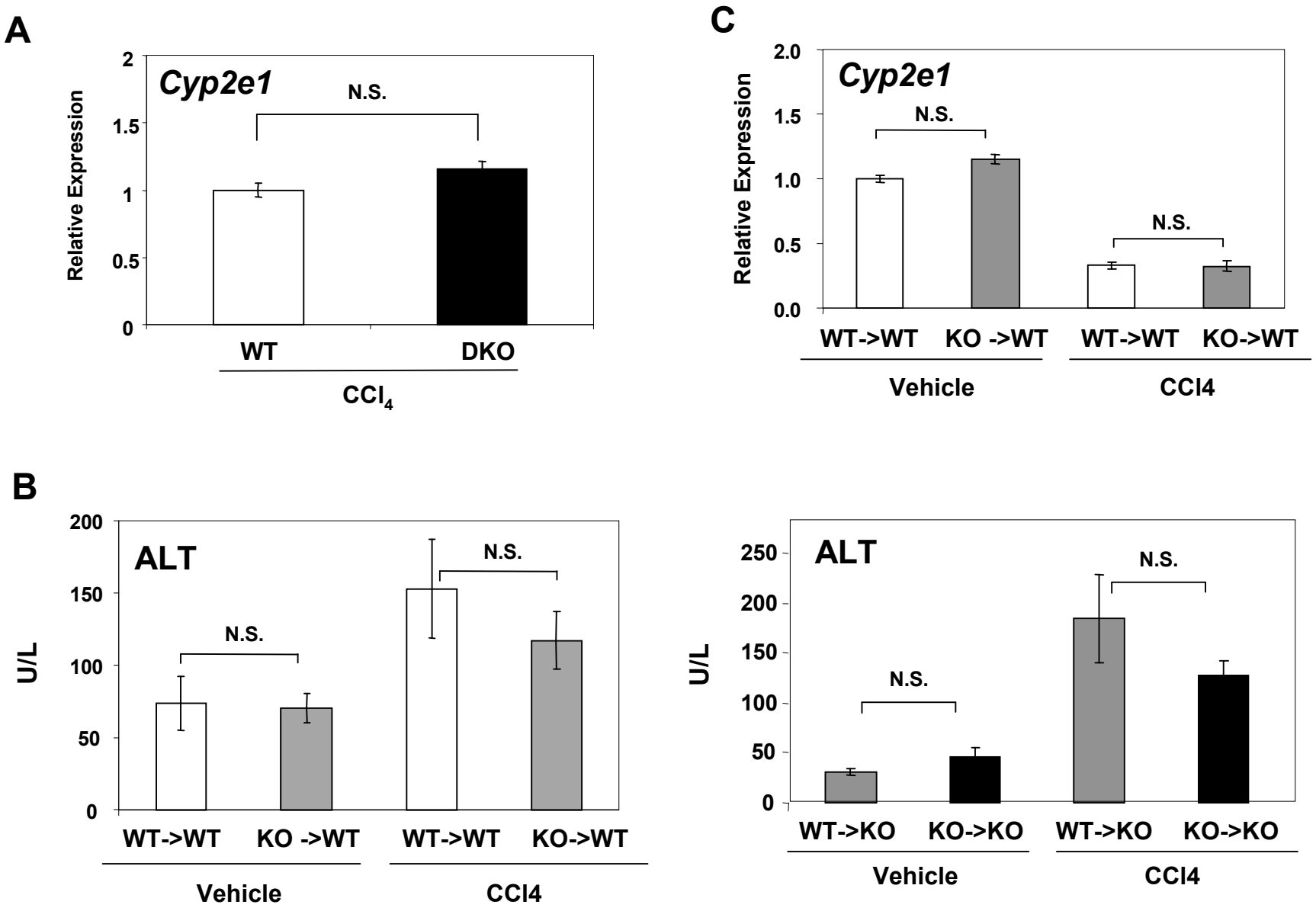

Beaven Suppl Figure 6